CORRELATION BETWEEN THE TENSILE STRENGTH AND CORROSION BEHAVIOR OF HEAT TREATED ZR-1.0NB ALLOY

TAE KYU KIM*, PYUNG SIK CHOI, SUNG KI YANG, CHONG TAK LEE and DONG SEONG SOHN
Korea Atomic Energy Research Institute
1045 Daedeokdaero, Yuseong, Daejeon 305-353, Republic of Korea
*Corresponding author. E-mail : tkkim2@kaeri.re.kr

Received February 20, 2008
Accepted for Publication May 9, 2008

The correlation between the tensile strength and corrosion behavior of Zr-1.0wt%Nb alloy heat treated at 480°C for up to 32 hours was evaluated. The tensile strength at 400°C was continuously reduced with an increasing heat treatment time, mainly due to a grain growth and a decreased area fraction of the precipitates. However, the corrosion resistance in an aqueous ammonia solution at 360°C was enhanced, mainly due to the formation of ß-Nb precipitates. It is thus concluded that a longer heat treatment time provides a better corrosion resistance while degrading the tensile strength.

KEYWORDS : Zr-1.0wt%Nb Alloy, Tensile Strength, Corrosion Behavior

1. INTRODUCTION

Metallic fuels can be utilized as nuclear fuel for advanced light water reactors due to their excellent thermal conductivity [1-4]. As a fabrication process of these metallic fuels, a billet composed of a metallic fuel and cladding material can be co-extruded by using their superior workability properties [5-7]. The plastically deformed metallic fuel rods should be heat treated to recover their mechanical properties degraded from the working. Thus, the heat treatment conditions involved have become a subject of interest.

The Zr-Nb alloys as a cladding material for the metallic fuels have been known to have excellent mechanical properties at high temperatures along with superior corrosion resistance [8-15]. The excellent mechanical properties of these alloys have been mainly attributed to the Nb-containing precipitates [8,9], while the superior corrosion resistance has been ascribed to the ß-Nb precipitates [10-12] and an equilibrium Nb concentration in the α-Zr matrix [13-15]. From these research results, it is thought that reliable mechanical and corrosion properties can be obtained when these alloys consist of not only the α-Zr matrix with an equilibrium Nb concentration but also ß-Nb precipitates. In a Zr-Nb binary system, the ß-Zr (~20 wt% Nb) and the ß-Nb (~80 wt% Nb) phases are precipitated above and below 610°C, respectively. It is well known that the ß-Zr precipitates usually play a detrimental effect on corrosion resistance due to the formation of cracks in a protective oxide layer during corrosion, while the ß-Nb precipitates act to generate enhanced corrosion resistance [10-12]. The Zr-1.0wt%Nb alloy, which contains a Nb concentration above its solubility (~0.6 wt%), should be heat treated below 610°C in order to form the ß-Nb precipitates. As a preliminary experimental result, a heat treatment at 580°C of an extruded Zr-Nb alloy induced improved corrosion resistance, but revealed a relative low tensile strength [16]. It is thus necessary to reduce the heat treatment temperature to less than 580°C in order to obtain an improved tensile strength along with a reliable corrosion resistance. In this study, an extruded Zr-1.0wt%Nb alloy is heat treated at 480°C, and its microstructure, tensile strength, and corrosion behavior are evaluated. Based on these results, a correlation between the tensile strength and corrosion resistance is discussed.

2. EXPERIMENTAL PROCEDURE

A Zr-1.0wt%Nb alloy rod (30 mm in diameter) was prepared by vacuum arc remelting (VAR), hot forging, hot extrusion, and heat treatment processes, and its chemical composition is given in Table 1. The alloy rod was machined to make a billet. The billet was heated in a

Table 1. Chemical Composition of the Zr-Nb Alloy (wt%)

Zr	Nb	Fe	Hf	C	H	O	N
Bal.	1.03	0.02	0.03	<0.001	0.0006	0.0461	0.0015

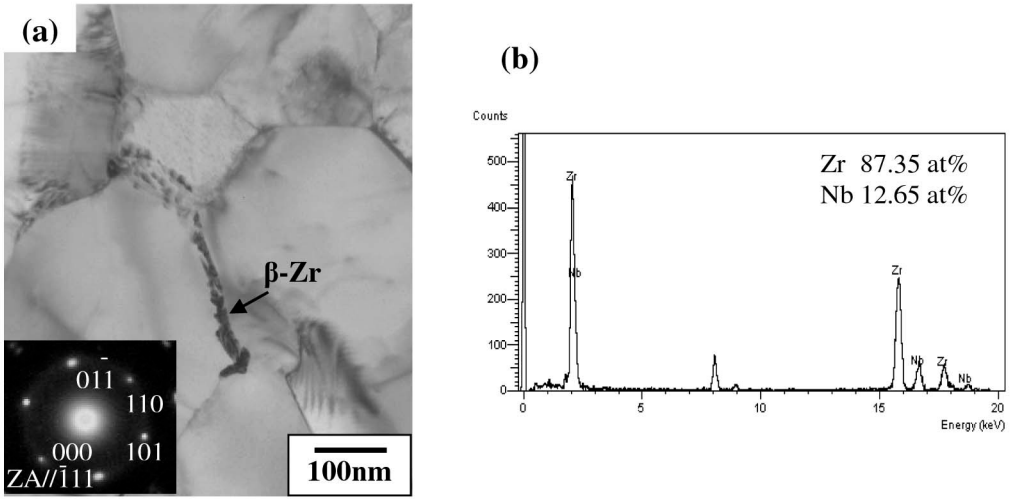

Fig. 1. TEM/EDS Results for the Precipitates of the Extruded Zr-Nb Alloy: (a) Bright Field Image, and a Selected Diffraction Pattern from Precipitation, and (b) Spectrum from Precipitation Arrowed in (a)

box furnace under an argon atmosphere at 700°C for 1 hour and was then extruded with an extrusion ratio of 30. The heat treatment of the extruded rod ($5 \times 5 \times 100$ mm) was carried out at 480°C for 3, 8, 16, and 32 hours in a vacuum, and this treatment was followed by a furnace cooling.

The tensile test specimen was prepared according to ASTM E8-04, and the tensile test was carried out at a strain rate of 10^{-4}/sec at 400°C. A Vickers microhardness was measured at a load of 0.3 kg_f. The corrosion tests were carried out in an aqueous ammonia solution adjusted to pH 10 under a pressure of 18 MPa at 360°C for 110 days by using a static autoclave. The corrosion behavior was determined by the gravimetric method with the exposure time.

The microstructures were observed by using a transmission electron microscope (TEM), and the elemental analyses on the precipitates were made by using an energy dispersive spectroscope (EDS) attached to a TEM. The TEM samples were prepared by a grinding up to 70 μm in thickness and were then electrolytically polished with a mixed solution of 90 vol.% ethanol and 10 vol.% perchloric acid by using a twin-jet polisher at -45°C. The area fraction of the precipitates was calculated by using an image analyzer (IA). The fractured surfaces after the tensile test were observed by using a scanning electron microscope (SEM). The concentration of hydrogen absorbed in a corroded sample was analyzed by using a hydrogen determinator. The hydrogen pickup fraction (F) was calculated by the following equation [17].

$$F(\%) = \frac{(\frac{m_o}{M_{Zr}} - \frac{\Delta m}{2m_0})M_{Zr}\frac{(C_H - C_{Hini})}{10^6}}{2M_H[\Delta m - (\frac{m_0}{M_{Zr}} - \frac{\Delta m}{2M_O})M_{Zr}\frac{(C_H - C_{Hini})}{10^6}]\Big/M_O} \quad (1)$$

where m_o is the sample mass before the corrosion test (g), C_{Hini} and C_H are the hydrogen concentrations in the initial and oxidized samples (ppm), respectively. In addition, Δm is the weight gain after the corrosion test (g), and M_O, M_H, and M_{Zr} are the molar masses of the oxygen, hydrogen, and zirconium (g/mol), respectively.

3. RESULTS AND DISCUSSION

3.1 Microstructure

Figure 1 shows the TEM/EDS studies for the precipitates of the extruded Zr-Nb alloy. Most of the

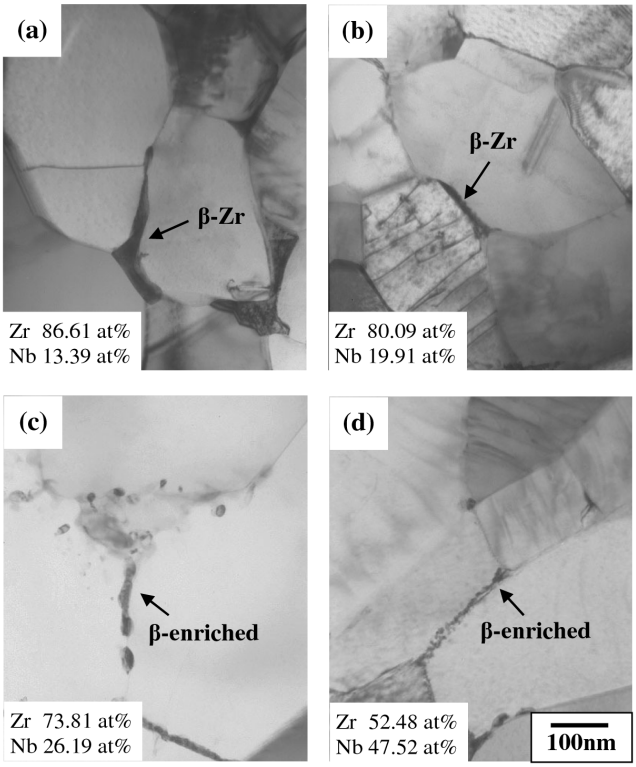

Fig. 2. TEM/EDS Results for the Precipitates of the Zr-Nb Alloys Heat Treated at 480°C for (a) 3, (b) 8, (c) 16, and (d) 32 Hours

precipitates were found in the grain boundary. The analysis of the SAD pattern indicated that the precipitation was the ß-Zr phase with a crystal structure of bcc (a=0.3545 nm), and its chemical composition was determined to be 87.35 at% Zr and 12.65 at% Nb. It is considered that the ß-Zr phase was precipitated during a pre-heating at 700°C for an extrusion. The TEM/EDS studies for the precipitates of the Zr-Nb alloy heat treated at 480°C for 3, 8, 16, and 32 hours are shown in Figure 2. Most of the precipitates were also found in the grain boundaries, and their Nb concentrations increased with an increased heat treatment time. The precipitates in the sample heat treated for 3 hours were identified as the ß-Zr phase with a Nb concentration of less than 14 at% (Fig. 2(a)). After a heat treatment for 8 hours, the Nb concentration in the precipitates increased up to about 20 at%, but most of the precipitates were still the ß-Zr phase (Fig. 2(b)). As the heat treatment time extended to 16 hours, enriched ß-Nb phases with a Nb concentration of more than 20 at% were found (Fig. 2(c)). The Nb concentration of the enriched ß-Nb phases in the sample heat treated for 32 hours increased further, up to 47.52 at% (Fig. 2(d)). The enriched ß-Nb phase represents the ß-Nb one with a crystal structure of bcc (a=0.3306 nm); however, its Nb concentration is less than 80 wt%, which is an equilibrium concentration of the ß-Nb phase. It is

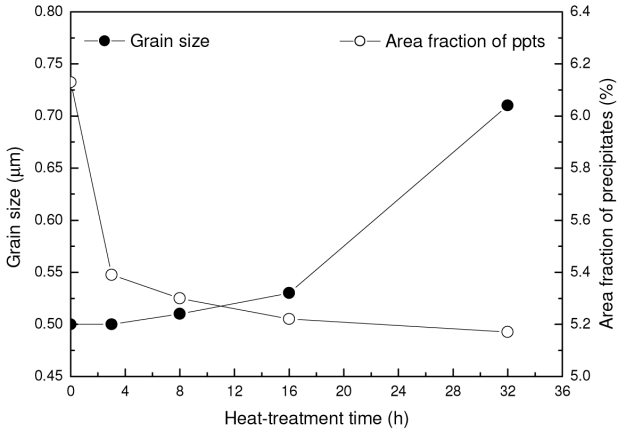

Fig. 3. Effects of a Heat Treatment on the Grain Size and Area Fraction of the Precipitates of the Zr-Nb Alloys

considered that the enriched ß-Nb phase was formed by a decomposition of the ß-Zr phase into the α-Zr and ß-Nb ones during a heat treatment at this temperature.

Figure 3 shows the effects of a heat treatment on the grain size and the area fraction of the precipitates of the Zr-Nb alloy. The grain size increased with an increased heat treatment time. However, the area fraction of the precipitates continuously decreased, mainly due to a decomposition of the ß-Zr phase into the α-Zr and ß-Nb ones.

3.2 Tensile Strength and Vickers Hardness

Figure 4 shows the tensile test results of the Zr-Nb alloy at 400°C. The yield and tensile strengths continuously decreased with an increasing heat treatment time at 480°C; however, they appeared to be improved by approximately 40%, as compared to the tensile

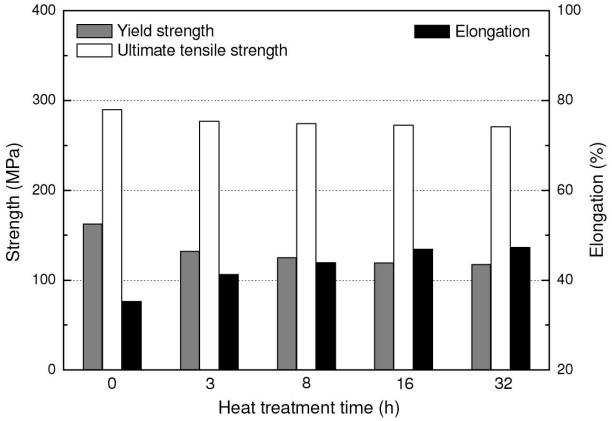

Fig. 4. Tensile Test Results of the Zr-Nb Alloys at 400°C

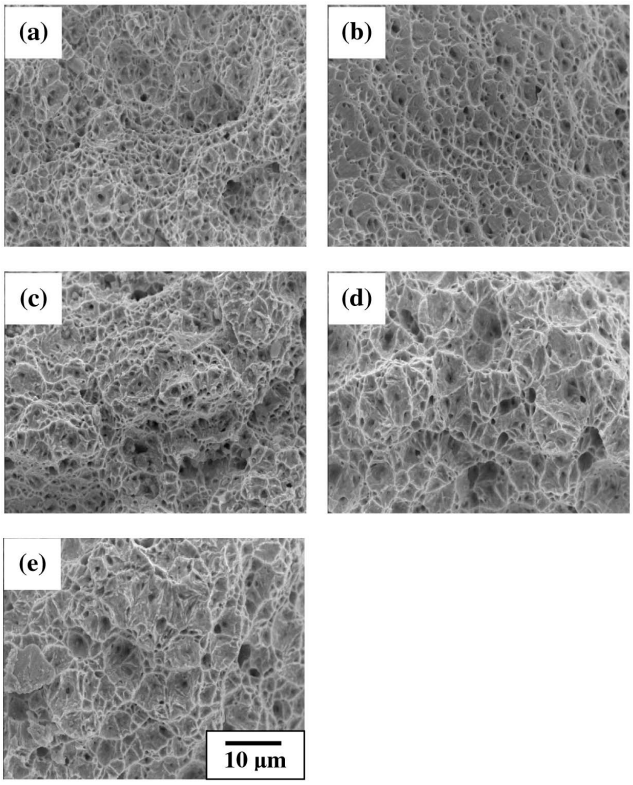

Fig. 5. SEM Fractographs after the Tensile Tests at 400°C of the Zr-Nb Alloys Heat Treated at 480°C for (a) 0, (b) 3, (c) 8, (d) 16, and (e) 32 Hours

strengths for the samples heat treated at 580°C [16]. The tensile strengths considered here depend on the grain size and amount of precipitates: a small grain size and a large number of precipitates increases the tensile strength, because a grain boundary and the precipitates act as obstacles to a dislocation movement under a stress condition. The heat treatment at 480°C induced a grain growth and a reduction in the area fraction of the precipitates (Fig. 3). It is thus considered that a decrease in the tensile strength by a heat treatment would be mainly attributed to a grain growth as well as to a reduction in the amount of precipitates. The elongation appeared to increase by a heat treatment. However, this alloy has superior ductility, because the elongation of the sample without a heat treatment was revealed at as high as 35%. These results could offer precise information in relation to the effects of a heat treatment on the tensile properties of the Zr-Nb alloy. The SEM fractographs after the tensile tests of the Zr-Nb alloys are shown in Figure 5. Similar dimples were found in the fractured surfaces of the extruded and heat treated samples, indicating a ductile rupture. It is thus concluded that a heat treatment negligibly affects the deformation mechanism of the Zr-Nb alloy at 400°C.

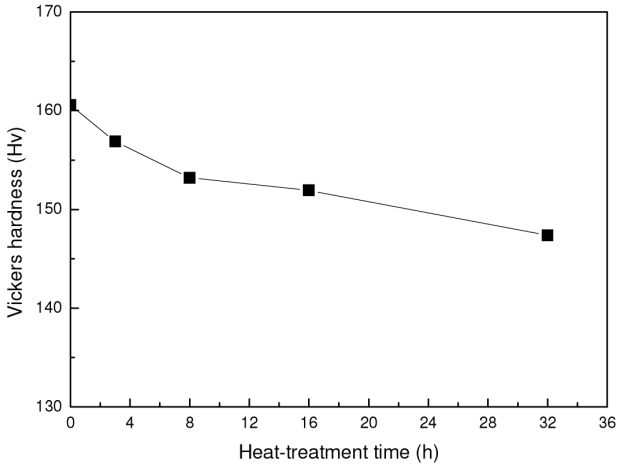

Fig. 6. Effect of the Heat Treatment Time on the Vickers Hardness of the Zr-Nb Alloy

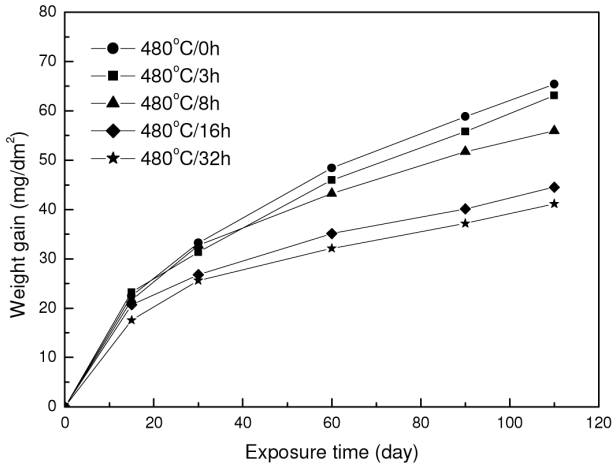

Fig. 7. Corrosion Behavior of the Zr-Nb Alloys in an Aqueous Ammonia Solution at 360°C

Figure 6 shows the effect of the heat treatment time on the Vickers hardness of the Zr-Nb alloy. The hardness decreased gradually in proportion to the heat treatment time. The hardness is mainly determined by the grain size and the amount of precipitates: a large grain size and a small amount of precipitates usually decreases the hardness. It is considered that a decrease in the hardness could be attributed to grain growth and a reduction in the amount of precipitates. These results coincide well with the tensile test results, which indicate that a heat treatment induces a reduction in the tensile strength (Fig. 4).

3.3 Corrosion Behavior

Figure 7 shows the corrosion behavior of the Zr-Nb

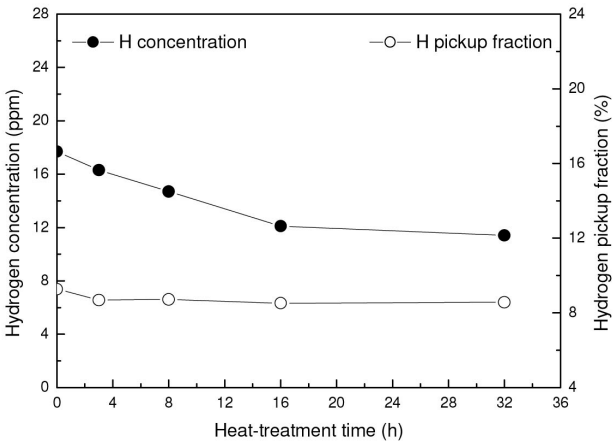

Fig. 8. Absorbed Hydrogen Concentrations and Hydrogen Pick-Up Fractions of the Zr-Nb Alloys after Corrosion in an Aqueous Ammonia Solution at 360°C for 110 Days

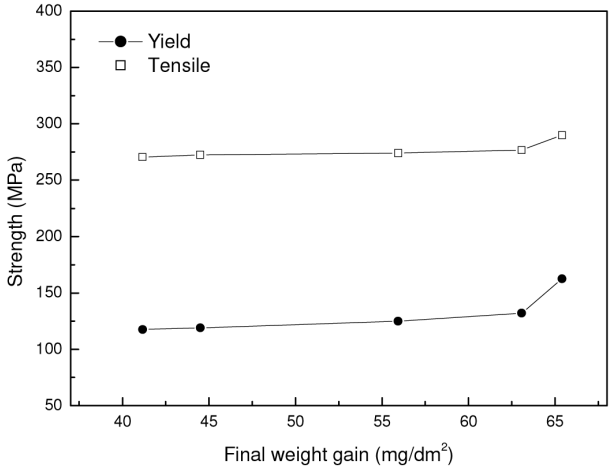

Fig. 9. Correlation between the Final Weight Gain after Corrosion at 360°C for 110 Days and the Tensile Strengths at 400°C

alloys in an aqueous ammonia solution at 360°C. The corrosion rate was rapid in the initial corrosion period, but decreased gradually after approximately 30 days. This behavior could be closely correlated with an increase in the thickness of a protective oxide layer. In addition, the corrosion rate was affected by the heat treatment time at 480°C, as the corrosion rate decreased with an increasing heat treatment time. The enhanced corrosion resistance could be mainly ascribed to a change in the composition of the precipitates; during a heat treatment at 480°C, the ß-Zr precipitates were continuously transformed to enriched ß-Nb precipitates (Figs. 1,2). These results coincide well with the previous studies, indicating that the corrosion resistance was enhanced when the ß-Zr precipitates transform to ß-Nb precipitates [10-12,16]. The absorbed hydrogen concentrations and hydrogen pickup fractions of the Zr-Nb alloy after a corrosion test for 110 days are shown in Figure 8. The concentration of the hydrogen absorbed in a sample during corrosion decreased with an increasing heat treatment time. The absorbed hydrogen concentration is closely correlated with the corrosion resistance: a better corrosion resistance usually provides a lower concentration of the hydrogen absorbed into the matrix. As a result, the hydrogen concentration decreased in proportion to the corrosion resistance, as shown in Figure 7. The hydrogen pickup fraction was determined to be about 8~9%. This result could be attributed to the characteristics of this alloy during corrosion in the aqueous ammonia solution.

3.4 Correlation between the Tensile Strength and the Corrosion Behavior

Figure 9 shows the correlation between the final weight gain after corrosion at 360°C for 110 days and the tensile strengths at 400°C. The yield and tensile strengths were continuously increased in proportion to the final weight gain, indicating that the improved tensile strength resulted in the accelerated corrosion rate. The extension of the heat treatment time at 480°C induced an enhanced corrosion resistance (Fig. 7) as well as a reduction in the absorbed hydrogen concentration (Fig. 8). It is thus concluded that a longer heat treatment provides a better corrosion property while degrading the tensile strength.

4. CONCLUSION

A Zr-1.0wt%Nb alloy was extruded at 700°C and then heat treated at 480°C for 3, 8, 16, and 32 hours. Most of the precipitates in the extruded sample were analyzed to be the ß-Zr phase with a crystal structure of bcc (a=0.3545 nm). These precipitates were continuously transformed to enriched ß-Nb precipitates during the heat treatment. The heat treatment also induced a grain growth as well as a decreased area fraction of the precipitates. The tensile strength at 400°C continuously decreased with an increasing heat treatment time, mainly due to grain growth and a reduction in the amount of precipitates. However, the corrosion resistance in an aqueous ammonia solution at 360°C was enhanced, mainly due to the formation of ß-Nb precipitates. It is concluded that a longer heat treatment time at 480°C provides a better corrosion resistance while degrading the tensile strength.

ACKNOWLEDGEMENT

This study was supported by the Korea Science and Engineering Foundation (KOSEF) and the Ministry of Education, Science, and Technology (MEST), Korea, through the National Nuclear Technology Program.

REFERENCES

[1] T. K. Kim, C. T. Lee, and D. S. Sohn, "Sintering Behavior of U-80 at.%Zr Powder Compacts in a Vacuum Environment", *J. Nucl. Mater*. **372**, 394 (2008).

[2] B. H. Lee, J. S. Cheon, Y. H. Koo, J. Y. Oh, J. S. Yim, D. S. Sohn, M. Baryshnikov, and A. Gaiduchenko, "Measurement of the Specific Heat of Zr-40 wt%U Metallic Fuel", *J. Nucl. Mater*. **360**, 315 (2007).

[3] J. S. Kim, Y. S. Jeon, S. D. Park, B. C. Song, S. H. Han, and J. G. Kim, "Dissolution and Burnup Determination of Irradiated U-Zr Alloy Nuclear Fuel by Chemical Methods", *Nucl. Eng. Tech*. **38**, 301 (2006).

[4] G. L. Hofman, L. C. Walters, and T. H. Bauer, "Metallic Fast Reactor Fuels", *Prog. Nucl. Ener*. **31**, 83 (1997).

[5] C. T. Lee, J. H. Park, T. K. Kim, U. J. Lee, B. S. Lee, and D. S. Sohn, "Thermal Stability of Co-Extruded U-Zr/Zr-Nb Alloys", *J. Nucl. Mater*. **373**, 275 (2008).

[6] S. M. McDeavitt, and A. A. Solomon, "Hot-isostatic Pressing of U-10Zr by a Coupled Grain Boundary Diffusion and Creep Cavitation Mechanism", *J. Nucl. Mater*. **228**, 184 (1996).

[7] K. Nakamura, T. Ogata, M. Kurata, A. Itoh, and M. Akabori, "Reactions of U–Zr Alloy with Fe and Fe–Cr Alloy", *J. Nucl. Mater*. **275**, 246 (1999).

[8] H. G. Kim, S. Y. Park, M. H. Lee, Y. H. Jeong, and S. D. Kim, "Corrosion and Microstructural Characteristics of Zr-Nb Alloys with different Nb Contents", *J. Nucl. Mater*. **373**, 429 (2008).

[9] S.W. Ha, J.Y. Huh, J.Y. Park, and Y.H. Jeong, "The Correlation of Annealing Parameter and Microstructures on Corrosion Characteristics and Mechanical Properties of Zr-1.0Nb Alloy", *J. Kor. Inst. Met.& Mater*. **39**, 1092 (2001).

[10] Y. H. Kim, J. H. Baek, and Y. H. Jeong, "Effects of Nb Contents and Final Annealing Temperatures on the Corrosion Characteristics of Nb-containing Zr Alloys", *J. Kor. Inst. Met. & Mater*. **40**, 1173 (2002).

[11] H. G. Kim, Y. S. Lim, M. Y. Wey, and Y. H. Jeong, "Effect of Niobium on the Microstructure and Corrosion Characteristics of Zr-xNb Binary Alloys", *J. Kor. Inst. Met. & Mater*. **37**, 584 (1999).

[12] Y. H. Kim, M. Y. Wey, J. H. Baek, and Y. H. Jeong, "Effects of Annealing Temperature and Sn Content on the Microstructure and Corrosion of Zr-1.5Nb-xSn Alloys", *J. Kor. Inst. Met. & Mater*. **42**, 167 (2004).

[13] Y. H. Jeong, H. G. Kim, and T. H. Kim, "Effect of ß Phase, Precipitate and Nb-concentration in Matrix on Corrosion and Oxide Characteristics of Zr–*x*Nb Alloys", *J. Nucl. Mater*. **317**, 1 (2003).

[14] Y. H. Jeong, K. O. Lee, and H. G. Kim, "Correlation between Microstructure and Corrosion Behavior of Zr–Nb Binary Alloy", *J. Nucl. Mater*. **302**, 9 (2002).

[15] Y. H. Jeong, H. G. Kim, D. J. Kim, B. K. Choi, and J. H. Kim, "Influence of Nb Concentration in the α-Matrix on the Corrosion Behavior of Zr–*x*Nb Binary Alloys", *J. Nucl. Mater.* **323**, 72 (2003).

[16] T. K. Kim, S. K. Yang, P. S. Choi, C. T. Lee, and D. S. Sohn, "Effects of Heat Treatment on the Tensile Strength and Corrosion Resistance of Extruded Zr-Nb Alloy", *J. Kor. Inst. Met. & Mater*. **44**, 823 (2006).

[17] M. Tupin, M. Pijolat, F. Valdivieso, M. Soustelle, A. Frichet, and P. Barberis, "Differences in Reactivity of Oxide Growth during the Oxidation of Zircaloy-4 in Water Vapour before and after the Kinetic Transition", *J. Nucl. Mater*. **317**, 140 (2003).